Received: 3 November 2022 | Revised: 28 June 2023 | Accepted: 29 June 2023

DOI: 10.1002/hyp.14939

RESEARCH ARTICLE

WILEY

Shallow and local or deep and regional? Inferring source groundwater characteristics across mainstem riverbank discharge faces

Adam B. Haynes[1] | Martin A. Briggs[1,2] | Eric Moore[1] | Kevin Jackson[1,3] | James Knighton[1] | David M. Rey[2] | Ashley M. Helton[1]

[1]Department of Natural Resources and the Environment, and the Center for Environmental Sciences and Engineering, University of Connecticut, Storrs, Connecticut, USA

[2]U.S. Geological Survey, Observing Systems Division, Hydrologic Remote Sensing Branch, Storrs, Connecticut, USA

[3]Appalachian Laboratory, University of Maryland Center for Environmental Science, Frostburg, Maryland, USA

Correspondence
Martin A. Briggs, U.S. Geological Survey, Observing Systems Division, Hydrologic Remote Sensing Branch, 11 Sherman Place, Unit 5015, Storrs, CT 06269, USA.
Email: mbriggs@usgs.gov

Funding information
U.S. Geological Survey; U.S. National Science Foundation Hydrological Sciences Program; U.S. National Science Foundation Division of Earth Sciences, Grant/Award Number: 1824820

Abstract

Riverbank groundwater discharge faces are spatially extensive areas of preferential seepage that are exposed to air at low river flow. Some conceptual hydrologic models indicate discharge faces represent the spatial convergence of highly variable age and length groundwater flowpaths, while others indicate greater consistency in source groundwater characteristics. Our detailed field investigation of preferential discharge points nested across mainstem riverbank discharge faces was accomplished by: (1) leveraging new temperature-based recursive estimation (extended Kalman Filter) modelling methodology to evaluate seasonal, diurnal, and event-driven groundwater flux patterns, (2) developing a multi-parameter toolkit based on readily measured attributes to classify the general source groundwater flowpath depth and flowpath length scale, and, (3) assessing whether preferential flow points across discharge faces tend to represent common or convergent groundwater sources. Five major groundwater discharge faces were mapped along the Farmington River, CT, United States using thermal infrared imagery. We then installed vertical temperature profilers directly into 39 preferential discharge points for 4.5 months to track vertical discharge flux patterns. Monthly water chemistry was also collected at the discharge points along with one spatial synoptic of stable isotopes of water and dissolved radon gas. We found pervasive evidence of shallow groundwater sources at the upstream discharge faces along a wide valley section with deep bedrock, as primarily evidenced by pronounced diurnal discharge flux patterns. Discharge flux seasonal trends and bank storage transitions during large river flow events provided further indication of shallow, local sources. In contrast, downstream discharge faces associated with near surface cross cutting bedrock exhibited deep and regional source flowpath

characteristics such as more stable discharge patterns and temperatures. However, many neighbouring points across discharge faces had similar discharge flux patterns that differed in chloride and radon concentrations, indicating the additional effects of localized flowpath heterogeneity overprinting on larger scale flowpath characteristics.

KEYWORDS
baseflow, evapotranspiration, groundwater discharge, groundwater-surface water interactions, heat tracing, river, riverbank storage, seepage

1 | INTRODUCTION

Approximately half of streamflow across the continental United States is supplied by discharge from groundwater (Scanlon et al., 2023), often focused to discrete high flow springs and seeps that arise from permeable geologic features (Marcelli et al., 2022). The water quality of groundwater discharging along riverbanks is influenced by source flowpath characteristics that can vary widely in spatial scale and average depth from the land surface (Barclay et al., 2020, Figure 1). The spatial distribution of discrete discharge points tends to be preferential rather than well distributed along the river corridor (Briggs & Hare, 2018), and numerous discharge points may cluster together to form extensive 'discharge faces'. Riverbank discharge points act as a unique window into the adjacent aquifer groundwater chemistry, which is often a reflection of accumulated land use legacies and geologic characteristics (Brookfield et al., 2021), and act as critical gateways for solute transport to surface water (Hester & Fox, 2020). While groundwater is often considered a relatively stable moderator of surface water variability (Leach et al., 2022), research over the past decade has highlighted the vulnerability of shallow groundwater flowpaths to climate and anthropogenic warming (Eggleston & McCoy, 2015; Kurylyk et al., 2014), dry periods (Zhi & Li, 2020), depletion by enhanced evapotranspiration (ET) (Condon et al., 2020), and other critical zone processes (Singha & Navarre-Sitchler, 2021). Alternatively, deeper groundwater flowpaths with long transit times may be more hydrologically and thermally stable but can perpetuate decadal land use contamination legacies through aquifers to surface waters, complicating water quality management strategies (Basu et al., 2022). Approaches that effectively and efficiently assess groundwater discharge source characteristics have important potential to improve river management decisions under current and future land use and climatic conditions.

For the purposes of this study, we focus on groundwater discharge along exposed riverbanks that have minimal hyporheic influence during low flow conditions, contrasting with other groundwater/surface water studies that primarily focus on bidirectional hyporheic exchanges and submerged groundwater discharge (e.g., Boano et al., 2010; Ocampo et al., 2006; Revelli et al., 2008). Prior research has conceptualized riverbank groundwater discharge along a spectrum of assumed complexity. On the simplified end, watershed- to basin-scale groundwater models often treat discharge as a net product of aquifer processes, considering groundwater as a well-mixed, single-sourced entity when it discharges to rivers at the scale of 100s metre grid cells or greater. At greater temporal complexity, Rice and Hornberger (1998) describe observed processes of older water being rapidly pushed out of riverbanks during recharge events, though they generalize groundwater flowpaths to individual discharge areas as similarly sourced (shown conceptually as the right bank on Figure 1b).

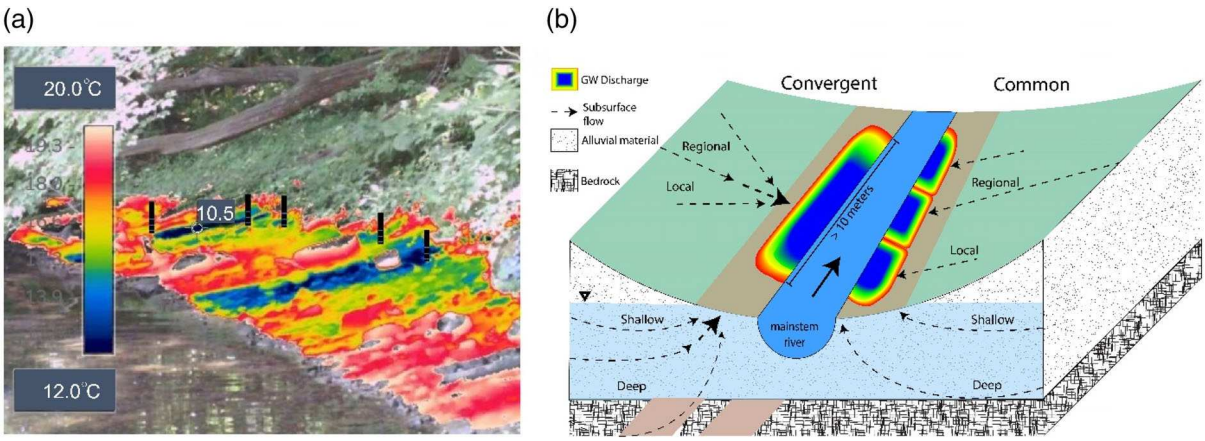

FIGURE 1 (a) Depicts thermal infrared (TIR) data across a riverbank discharge face overlaying a photo of the terrain (field site River Island 5). The TIR data show the characteristic cold thermal signature of groundwater emergence in summer at preferential discharge points (cold, blue) with locations of vertical temperature profiles indicated by black bars. (b) Shows differing conceptual models of groundwater flowpaths to riverbanks, with varied characteristic flowpaths converging tightly in space to one face on river left and common groundwater sources feeding individual faces on river right.

Representation of groundwater discharge at riverbanks has also taken on more dynamic and complex conceptualizations. Modica (1999) describes a tight spatial convergence at discharge faces of vastly different aged groundwater flowpaths (summarized conceptually as the left bank on Figure 1b). Characteristics range from younger, shorter flowpaths higher on the bank, to older, longer flowpaths compressed toward the river. That concept was based primarily on particle tracking paired with groundwater flow models; supporting field data has been less clear. While both common and convergent conceptualizations and various combinations thereof may be circumstantially valid, the way groundwater flowpaths express themselves among and within mainstem river discharge faces remain largely under evaluated.

Although groundwater discharge faces are relatively contiguous features along mainstem rivers, measurements of groundwater seepage rates are often further focused to preferential discharge points (PDPs) of relatively high discharge rates occurring within extensive faces (Briggs et al., 2022, Figure 1a). Using fundamental hydrologic principles related to Darcy's Law, temporal discharge flux records can indicate high-level source groundwater characteristics at the PDP scale, potentially parsing deep from shallow and local from regional flowpaths. For example, ET and seasonal decline of the water table within the critical zone are expected to most directly impact discharge rates from shallow groundwater flowpaths (Singha & Navarre-Sitchler, 2021). Direct measurements of submerged discharges in a lake indicate diel variation on the order of 10% that was attributed to ET pumping of source groundwaters (Rosenberry et al., 2013), and more broadly ET is recognized as an important depletion mechanism of shallow groundwater storage (Condon et al., 2020; Nichols, 1994; Rosenberry & Winter, 1997; Shanafield et al., 2015). Therefore the temporal flux rate patterns of PDPs sourced by shallow groundwater, which are controlled by changing lateral hydraulic head gradients, should reflect those source flowpath processes as characteristic subdaily to seasonal variability. Additionally, PDPs that show discharge flux reversals (bank storage) during high river flow events are more likely to be sourced by short, local flowpaths where the lateral hydraulic gradient is strongly impacted by variable river stage and riparian water table elevation compared to long, regional flowpaths with more stable gradients (Briggs et al., 2018).

Despite the characteristic imprint of near surface critical zone processes on groundwater discharge flux rates, vertical flux records have not been previously used to infer groundwater sources to riverbank discharges, due in part to monitoring limitations. Seepage meters cannot readily be installed along exposed riverbanks above the waterline and typically do not track temporal changes in water flux at high resolution unless using automated methods (e.g., Rosenberry et al., 2013). And while vertical heat tracing methods are more conducive to installation in saturated sediments along exposed riverbanks, common methods of analysis based on diurnal temperature signals alone do not well-capture subdaily and abrupt changes in flux rate (Lautz, 2012). Numerical methods can accurately capture rapid and variable changes in flux rate, but typically only when paired with vertical pressure data (LeRoux et al., 2021) or via manual calibration of multiple model stress periods, and therefore the analysis is difficult to scale to many measurement locations at seasonal timescales. Recent application of spectral and recursive estimation Kalman Filter-based approaches may allow accurate tracking of rapid vertical flux changes due to storms, dam operation, and other subdaily to seasonal dynamics (McAliley et al., 2022; Sohn & Harris, 2021). McAliley et al. (2022) reformulated the one-dimensional convection/conduction equation as a linear time-varying state space model using a spatial finite difference approximation and matrix exponential for the solution as a function of time. Because this rapid new method does not rely on diurnal signal characteristics to calculate discharge flux, there is potential for more accurate depiction of variable flux rates, particularly at the subdaily timescale, and during high flow and storm events when natural temperature signals are muted and distorted. Additionally, the recursive estimation methods use information from adjacent time steps to refine current time flux estimates allowing more certain tracking of multiscale groundwater flux changes (McAliley et al., 2022).

The goals of our study were methodological and hydrologic process based. First, we extensively demonstrate the new recursive estimation heat tracing technique for tracking multiscale temporal discharge flux variability. Then, we develop a transferrable approach to use multi-month PDP flux records to infer general source groundwater flowpath characteristics among and within individual riverbank discharge faces. This approach is applied at 39 observed PDPs embedded within larger discharge faces along the 5th order Farmington River, Connecticut, United States. A spectrum of recently developed groundwater flow models of the Farmington River corridor simulate source groundwater discharge flowpaths ranging from local riparian and floodplain scale (10s–100s of metres) to regional scale (multiple kilometres, Barclay et al., 2020). Average simulated source flowpath depths across the selected models ranged from a median of 6.2 to 21.8 m. This range spans the upper, near surface zone most strongly impacted by near surface critical zone ET, recharge, and heat exchange processes, here generally termed 'shallow' groundwater, to deeper groundwater with reduced short-term variability. However, the groundwater flow models of Barclay et al. (2020) do not have fine enough spatial resolution to assess variability in groundwater sources at the scale of observed Farmington riverbank discharges (Barclay et al., 2022), nor the necessary geological complexity to explore specific PDP sources. Here, temporal groundwater flux pattern analyses were used to classify PDPs as having shallow versus deep and local versus regional groundwater sources, with a focus on shallow/local and deep/regional classification pairings. We assume that while deep groundwater must, by definition, travel through shallow sediments immediately prior to discharge, transit time through those sediments to PDPs is quick, such that shallow groundwater characteristics are not adopted, and deep source groundwater can be identified. Conservative dissolved chloride (Cl^-) and metrics of stable isotopes of water were used to further infer common or convergent groundwater sources (i.e., Figure 1b) while dissolved radon gas was used to infer fine scale flowpath geologic heterogeneity. Finally, we assess the river corridor geologic framework that may control source groundwater characteristics using recently collected passive seismic and towed transient electromagnetic data to 'scale up' our point scale observations of preferential riverbank discharge to a river corridor geologic

context. This study provides a unique in-depth look at discharge flux patterns from exposed riverbanks across the growing season and change in water year (4.5 months) at 39 discrete preferential flow points located across larger discharge faces, yielding new insight into the coupling of groundwater and mainstem rivers.

2 | METHODS

2.1 | Study area

The Farmington River watershed is a 1571 km^2 mixed land use watershed with underlying bedrock generally composed of New England crystalline rock, Mesozoic sandstone, and Newark Supergroup basalt (Olcott, 1995). We focus this study on five groundwater discharge faces operationally defined as laterally extended (>10 m) discharge features along riverbanks at or above the water line with multiple embedded PDPs as indicated with thermal infrared (TIR) and direct measurements. The study faces are located along two reaches of differing hydrogeology along the fifth-order mainstem of the Farmington River, a major tributary to the Connecticut River located in northwestern Connecticut (Figure 2a). The River Island reach is located along the west-to-east flowing portion of the Farmington River downstream of the Tariffville Gorge in an area where the river flows approximately normal to bedrock strike, down dip (Figure 2b). Median depth to bedrock measured at six locations with passive seismic methods along the River Island reach seepage faces was 14.5, 2.3 m SD (Jackson et al., 2023). The River Island reach banks generally comprise highly permeable glacial deposits of sand and gravel and adjacent land use includes residential and forested land with a mix of hardwood and conifer tree species. The upstream Alsop Meadows study reach is located along the south-to-north flowing portion of the Farmington River (Figure 2c), with surficial geology dominated by loamy fine sand glacial till. Along the Alsop reach, the river generally runs along bedrock strike with relatively thick sediment accumulation. Mean depth to bedrock measured at 10 measurement locations with passive seismic techniques was 23.2, 5.5 m SD

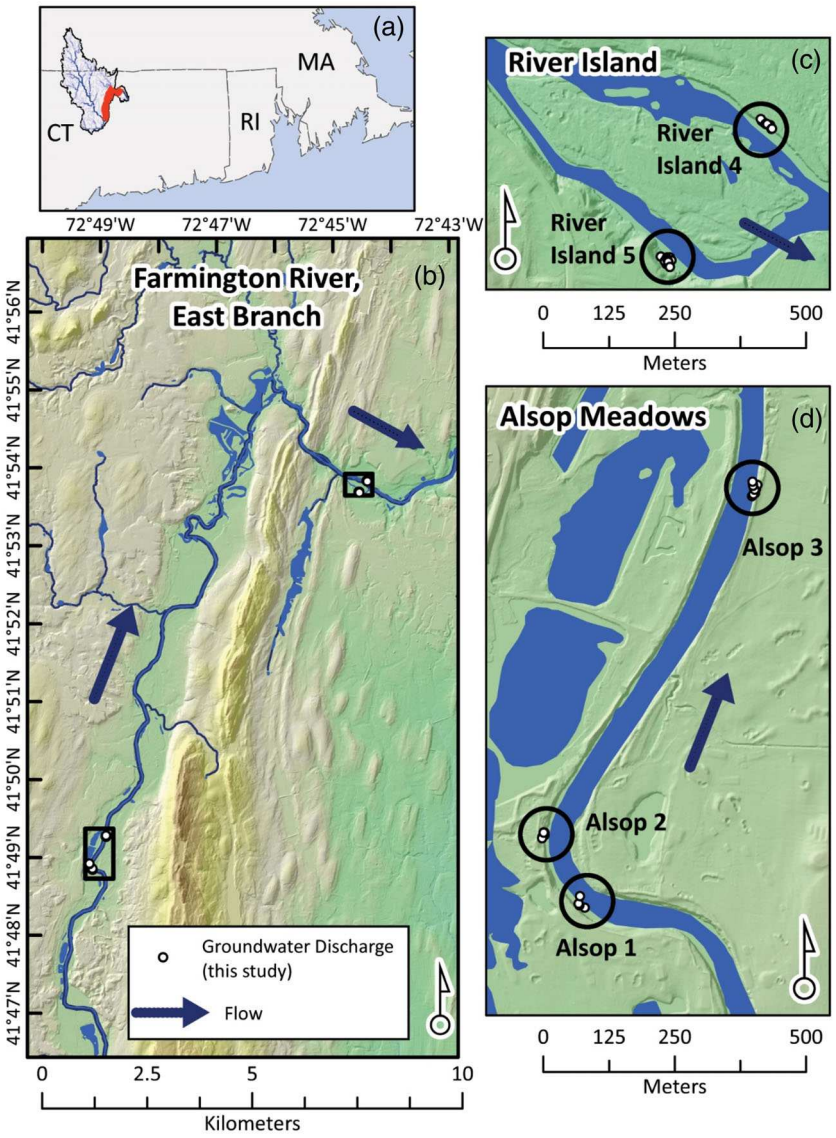

FIGURE 2 The study was conducted in the (a) Farmington River watershed located in Connecticut and Massachusetts, United States, (b) specifically at clusters of riverbank preferential discharge points (PDPs) along two sections of the East Branch of the Farmington River at the (c) River Island and (d) Alsop Meadows reaches. Map layers in the form of hillshade rasters and digital elevation models were derived from Connecticut Lidar Data downloaded from the Connecticut Department of Energy and Environmental Protection (CT Eco, 2016) and stream networks were provided by Barclay et al. (2020).

(Jackson et al., 2023). Near-river land use includes a golf course, cropland, and the Nod Brook Wildlife Management Area which contains several large shallow ponds bordered by phreatic trees. Bank sediments along this reach are mapped generally as high permeability soils with finer scale variability that has not been found to control the occurrence of PDPs (Briggs et al., 2022).

2.2 | Site selection and instrumentation

There has been rapidly growing use of TIR imagery to efficiently locate groundwater discharge for the inference of subsurface flowpath characteristics (e.g., Marcelli et al., 2022). Groundwater discharge faces in this study were selected based on TIR surveys along a 26.5 km stretch of the mainstem of the Farmington River (Moore, Jackson, et al., 2023) via the process described by Briggs et al. (2022). We used handheld TIR cameras (E8, FLIR Systems) from watercraft to identify thermal anomalies along the riverbanks associated with bankside groundwater discharge, along with direct riverbank temperature measurements and visual observations of physical discharge features. Instrument emissivity was set to 0.98, consistent with freshwater in the summer (Handcock et al., 2012), and viewfinder temperature ranges were set to span stream and groundwater temperatures to highlight cold anomalies. Groundwater temperatures were generally 9–12°C within the Farmington River watershed (Barclay et al., 2022), creating distinctive thermal targets associated with PDPs during warm weather (e.g., Figure 1a).

Each mapped discharge face contained numerous PDPs at varied distances from the low river water line embedded in a larger bank area of more diffuse groundwater seepage. Temperature measurements (direct and TIR) and supporting observational data (visible bank saturation and flow) were used to select a subset of PDPs for installing vertical temperature profilers. The profilers each contained three temperature loggers (Thermochron iButton model #1922L) at 0.01, 0.07, and 0.11 m depths where daily temperatures are most dynamic in areas of discharge. Following Briggs et al. (2014), temperature logger spacing was optimized for the quantification of groundwater flux out of the bank (upward flow) over time while providing flexibility to also quantify downward flux into the bank (bank storage events) that could occur at a high river stage. Temperature profilers were installed at 40 PDP sites to capture daily, river flow events, and seasonal discharge vertical water flux dynamics from mid-June 2020 to November 2020.

2.3 | Analytical and recursive estimation 1D discharge flux modelling

Vertical temperature profiler data collected within the five study riverbank discharge faces were used to quantify vertical discharge flux over time at each PDP. We measured saturated sediment thermal conductivity and heat capacity in the field with a TEMPOS Thermal Property Analyzer (TEMPOS, Meter Group, Inc., Pullman, WA, United States) at multiple points across each discharge face for use in 1D discharge flux modelling. The TEMPOS probe prongs were pressed directly into the saturated sediments of the discharge points to minimize sediment disturbance and measured thermal parameters were averaged for each face as described by Haynes et al. (2023). Vertical discharge flux patterns were estimated over time using the extended Kalman Filter (EKF) recursive estimation approach of McAliley et al. (2022) applied 0.01, 0.07, and 0.11 depth temperature sensor data. The 'Hatch Amplitude' attenuation analytical model run with VFLUX2 software (Irvine et al., 2015) was also initially applied but resulted in spurious results during storm events when natural diurnal signals were non-ideal, so the VFLUX2 results are not shown here but are included in the data release (Haynes et al., 2023). Unlike some analytical fluid flux estimates based on the vertical propagation of natural temperature signals (e.g., Kampen et al., 2022; Luce et al., 2013; Sohn & Harris, 2021), the EKF method does not provide estimates of effective streambed thermal diffusivity, a critical parameter for the prediction of diffusive (conductive) sediment heat fluxes. Instead, the EKF method requires the parameterization of sediment thermal conductivity and sediment volumetric heat capacity to solve the 1D convection/conduction partial differential equation formulated as a state space model (Constantz, 2008; McAliley et al., 2022). To address this uncertainty thermal parameters at each PDP were independently measured using the TEMPOS instrument, as described above.

The EKF method was used to recursively estimate specific discharge in discrete time when temperature measurements were acquired (i.e., hourly) at each PDP over 4.5 months. The variance of the EKF predicted 1D flux can be obtained from the diagonal elements of the state covariance matrix, consequently, confidence intervals can be calculated from EKF predictions using the posterior state covariance matrix. Kalman Filters have recently been more commonly applied to hydrologic problems (e.g., Kang et al., 2018; Shapiro & Day-Lewis, 2021, 2022; Sun et al., 2016). The methodology used here has been previously tested on both synthetic and field data in McAliley et al. (2022) where EKF methods were shown to converge to step changes in synthetic discharge data on sub-daily timescales, and residuals between observed (i.e., field observations) and estimated (i.e., EKF predictions) temperature observations were generally within 0.1°C, consistent with expected measurement precision. Further information on the numerical implementation, comparisons to synthetic and field observations, as well as links to open-source code can be found in McAliley et al. (2022).

2.4 | Groundwater sample collection and analysis

We collected monthly (mid-June 2020 to October 2020) groundwater chemistry samples at each PDP within the study discharge faces where vertical temperature profilers were installed. Porewater samples were obtained with small piezometers (PushPoint (PPX36), MHE Products, East Tawas, MI) installed directly into the points of discharge. We inserted the sampler 20 cm into the sediment and developed the piezometers with a three-way valve manifold and 60-mL syringe until minimal sediment was visually present in extracted water. We extracted 120 mL of water to measure the field parameters of dissolved oxygen, specific conductance, and temperature using a

handheld multimeter (YSI 6000, YSI Inc., Yellow Springs, OH). Another 120 mL of discharge water was collected in an HDPE bottle that had been washed with phosphate-free soap and triple-field rinsed. Samples were refrigerated, syringe filtered (Whatman GF/F) within 24 h of collection, and frozen until laboratory chemical analysis at the Center for Environmental Science and Engineering, Storrs, CT. We measured anion concentrations by ion chromatography (Dionex ICS 1100). The measured Cl^- concentrations are presented for this investigation of seepage face groundwater flowpath sources.

During the last sampling event in October 2020, we collected and filtered 60-mL samples from PDPs for analysis of $\delta^{18}O$, $\delta^{2}H$, and dissolved radon-222 (^{222}Rn) gas. Stable isotopes in water samples were stored with no bottle headspace, wrapped in parafilm, and refrigerated until processing the Center for Environmental Science and Engineering, Storrs, CT. The field filtered water samples were run on a Picarro L2130-i in high precision mode (0.025/0.1‰ for $\delta^{18}O/\delta D$) with three water standards spanning the range of collected samples. Line conditioned excess (lc-excess), indicating the degree of evaporative fractionation, was computed from the local meteoric water line (LMWL, Equation 1) established for Storrs, CT with 109 daily precipitation samples collected across 2020 and 2021 (Knighton, 2021).

$$\text{lc-excess} = \delta^{2}H - 7.519\left(\delta^{18}O\right) + 10.123 \quad (1)$$

Levels of ^{222}Rn in groundwater are generally dependent on sediment and rock type to which groundwater is recently exposed, the surface area of those materials, and the groundwater residence time (Hoehn & von Gunten, 1989). Given the short half-life of ^{222}Rn of 3.8 days, radon concentrations predominantly reflect geologic exposure within a few weeks transit time from aquifer to discharge zone. We collected 250 mL of unfiltered discharge water for ^{222}Rn sampling using our push point sampler with no headspace. Data were analysed within ~3 days of sample collection using a RAD7 instrument (DURRIDGE Company, Inc., Billerica, MA), and radioactive decay corrections were performed to account for the elapsed time since sample collection. Groundwater chemical constituent data used for this study are available from Moore, Haynes, et al. (2023).

2.5 | Source groundwater inference

We designed the discharge face groundwater categorizations defined in Table 1 to assess the degree of common versus convergent flowpath sources to PDPs across each groundwater discharge face based primarily on multiscale temporal groundwater flux patterns. The most objective measure of shallow groundwater influence was the existence of pronounced diurnal pumping flux patterns (exceeding 0.03 m/day signal amplitude) as quantified with dynamic harmonic regression analysis applied to the EKF model output. We highlight PDPs as shallow, locally sourced groundwater when diurnal pumping was found in conjunction with both metrics of local-scale groundwater flowpaths - the existence of seasonal groundwater flux patterns and flux direction reversal during high river flow events. Shallow/local PDPs are contrasted with PDPs that showed little systematic diurnal discharge flux variation and lacked seasonal patterns and flux reversals, indicating deeper, more regional groundwater sources. Seasonal PDP temperature patterns, Cl^- concentrations, and the lc-excess synoptic provided further insight regarding common or convergent groundwater sources.

TABLE 1 Summary of the attributes used to categorize groundwater discharge face source flowpaths.

	Category definitions	
Metrics	**Shallow**	**Deep**
Diurnal discharge pattern	Pronounced diurnal discharge rate pattern likely caused by evapotranspiration (>0.03 m/day).	Lack of diurnal rate pattern based on measured discharge rate signal amplitude (<0.03 m/day).
Max–min temperature difference	Indication of a seasonal shift in groundwater discharge temperature of >6°C.	Indication of season shift in groundwater discharge temperature of <3°C.
	Local	**Regional**
Seasonal discharge pattern	Enhanced discharge flux in early summer and later fall, weak summer discharge flux.	Lack of clear seasonal discharge flux pattern.
Riverbank storage	Significant discharge flux rate reversal (river water into bank) for at least one contiguous day (95% CI).	Lack of significant discharge flux rate reversal (95% CI).
	Common	**Convergent**
Chloride concentration	The SE of mean for all PDP locations were within range of one another.	The SE mean for one or more PDP locations was outside the range of one another.
lc-excess	The variance of the lc-excess values of a single discharge face is less than or equal to the variance of the dataset as a whole.	The variance of the lc-excess values of a single discharge face is greater than the variance of the dataset as a whole.

We examined the streambank temperature time series at the deepest sensor (~11 cm) for evidence of seasonal temperature shifts in discharging groundwater temperature indicative of shallow groundwater (e.g., Hare et al., 2021). More stable seasonal temperature regimes indicate deeper groundwater sources, emanating from below the ~6 m shallow zone of pronounced vertical annual temperature signal propagation (Constantz, 2008). Although 11 cm is inherently a shallow measurement, short term land surface temperature changes are typically strongly muted by that depth in preferential groundwater discharge zones (Briggs et al., 2014), so we assumed observed seasonal temperature patterns primarily reflected source groundwater temperature dynamics. The difference between the running 7-day maximum and

minimum temperature time series over the 4.5-month deployments was used to indicate the presence of seasonal patterns. The average 7-day max–min mean difference among the discharge faces was ~5°C, thus we considered a max–min difference >6°C as an indication of a shallow groundwater flowpath. PDPs with a max–min difference <3°C indicated a more seasonally stable deep groundwater signature. Source groundwater depths of locations with average seasonal temperature change between 3 and 6°C were considered inconclusive. Overall, the seasonal max–min temperature difference was considered the most qualitative of all the metrics determined for this study due to the assumed thresholds and the fact that low-flux discharge can also show seasonal temperature shifts as impacted by downward conduction of local seasonal heat, regardless of source groundwater depth.

We applied the EKF recursive estimation discharge flux modelling methods to the raw PDP temperature data from 39 locations (one PDP was dropped due to clear times of desaturation) and proceeded with in-depth analysis of the EKF model results. As a primary indicator of shallow groundwater sources, we inspected the EKF temporal water flux records for diurnal patterns that might be driven by ET along relatively shallow flowpaths accessible by floodplain phreatophyte vegetation and/or wetlands and ponds adjacent to the river. To do this, we used the dynamic harmonic regression approach of 'Captain Toolbox' (Young et al., 2010) to the EKF modelled discharge flux patterns to assess whether diurnal signals existed, and if so, to quantify their amplitude over time. This discharge flux signal processing approach created a quantitative metric of (presumed) upgradient ET influence. Analysis of the harmonic regression power spectral output for all sites was used to determine signal amplitude threshold for 'substantial' diurnal discharge flux patterns of 0.03 m/day, where amplitude is defined as half of the total daily discharge flux signal range. Sites with an average diurnal pumping discharge signal of at least 0.03 m/day amplitude across the measurement period were classified as having a shallow groundwater source (Table 1).

The other short-term discharge flux process used as a source groundwater inference metric was evidence of flux reversals, otherwise known as bank storage, that can occur during episodic high river flow events even when the general groundwater hydraulic gradient is toward the river (Shuai et al., 2019). We assumed that significant reversals of flux direction (outside the EKF model results 95% confidence interval) indicated shorter, local discharge flowpaths. The lateral hydraulic gradient is more sensitive to meter-scale changes in river surface elevation compared to long, kilometre-scale regional discharge flowpaths. Stability in discharge flux patterns of presumed deep/regional discharges has been noted relative to local hillslope streambank discharge in previous studies (Rosenberry et al., 2016). In hydrogeologic settings that differ from the Farmington River corridor, local flowpaths may be deeper than the phreatophyte rooting zone and zone of annual temperature signal fluctuation if soils are highly permeable along contributing hillslopes as noted by Briggs et al. (2020).

We examined all groundwater discharge flux time series for patterns (Figure 3) indicative of local/shallow versus regional/deep source groundwater characteristics, where the former is expected to be more sensitive to seasonal water table fluctuations. Local groundwater flowpaths can display increased flux in the spring and fall months and decreased flux in the summer months due to the change in water table and river surface levels. Deeper groundwater is less impacted by such seasonal water table drawdown (Burns et al., 1998). Pronounced seasonal flux patterns were identified for this study as locations that started the early summer measurement period with several weeks of sustained discharge, followed by a mid-late summer circumneutral flux period (flux rate not significantly different than zero), followed by a late fall sustained increase back to significant discharge rates (Table 1).

To augment the inference of source groundwater based on multi-scale groundwater flux rate patterns, we collected Cl^- and stable water isotope data. We used the mean and SE of seasonal Cl^- concentrations ($n = 5$; monthly samples from June to October) to indicate whether the groundwater source among PDPs of an individual face were common or converging (Table 1). The mean of the monthly Cl^- data ± the SE created ranges that were compared between PDPs across each discharge face. If two or more PDPs lacked overlapping Cl- ranges, the source groundwater flowpaths of the face were inferred to be convergent. Because anthropogenic sources frequently disrupt natural Cl^- levels (Cassanelli & Robbins, 2013), we decided it would not be practical to attempt groundwater age or travel time estimates based on our Cl^- samples and instead use the parameter to indicate source flowpath heterogeneity.

Isotopic differences between groundwater samples and local precipitation can be used to distinguish between local and regional flowpaths in mountainous regions (Springer et al., 2017). However, the muted topography of western Connecticut is not conducive to such analysis. Instead, the lc-excess metric (Equation 1) derived from stable isotopes of water was used to determine if the contributing groundwater flowpaths had been directly influenced by evaporation via upgradient exchange with floodplain ponds and wetlands, as surface water features exist across the Farmington River floodplain. The variance of lc-excess metrics across individual discharge faces was calculated and compared to the variance of the larger PDP populations from the study to assess discharge face-scale variability in lc-excess. If the variance along an individual discharge face was greater than that of all remaining PDPs, the face was characterized as having convergent flowpaths. Concentrations of ^{222}Rn are potentially controlled by fine scale geologic differences (Bourke et al., 2014), which may be expected to vary even among groundwaters of generally common sources. Therefore, we did not use ^{222}Rn for source groundwater characterization (not included in Table 1), and instead the ^{222}Rn provided general insight into flowpath geologic context.

3 | RESULTS

The riverbank discharge faces in this study show signs of converging groundwater flowpaths sourcing PDPs based on defined attributes (Table 1). Overall the Alsop Meadows sites indicated a prevalence of shallow/local groundwater sources compared to the downstream River Island sites that displayed characteristics of deeper/regional source groundwater metrics.

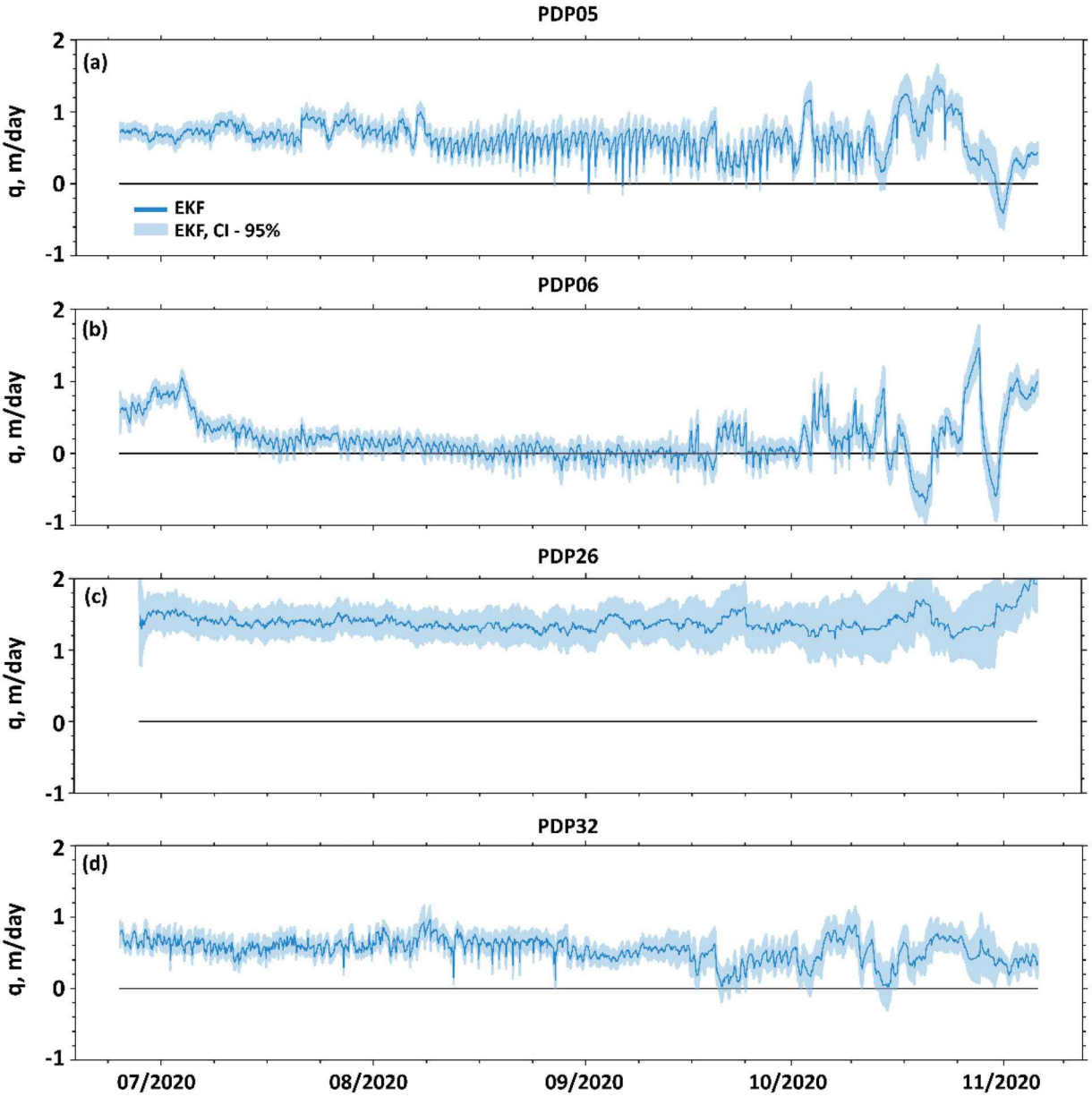

FIGURE 3 Discharge flux patterns for four example preferential discharge point (PDP) locations as modelled by the extended Kalman filter (EKF) method, where discharge (upward flow direction) is indicated by positive values for ease of interpretation. (a) Is a PDP with a clear diurnal flux pattern and one flow reversal event, and (b) is similar but also shows a seasonal trend with circumneutral flux mid to late summer. (c) Exemplifies the deep/regional flux pattern with relatively little diurnal or seasonal variability, and (d) shows a regional discharge signal with minor diurnal variability.

3.1 | Seepage face descriptions

Three distinct and spatially extensive discharge faces were mapped along the Alsop Meadows reach ranging from 11 to 27 m in length laterally along the riverbanks (Figure 2d). Alsop faces 1 and 2 were located along the downstream left riverbank on the outer edge of a large meander bend and bisected by a small surface tributary to the river. There were several surface water ponds in the adjacent upgradient floodplain, and the Alsop 1 discharge face was in the closest proximity to a golf course. Alsop 3 was ~800 m downstream along the right-side riverbank in a relatively straight stretch of river channel adjacent to farm fields. Four PDPs were mapped across Alsop 1 (PDP1-4), 6 PDPs were mapped across Alsop 2 (PDP5-10), and 10 PDPs across Alsop 3 (PDP11-20).

Further downstream along the River Island, two extensive discharge faces (i.e., 29 and 26 m in length along respective riverbanks) were mapped along the left bank of the main channel (River Island 4) and right bank of the island side channel (River Island 5) at approximately the same downstream distance (Figure 2c). A total of 20 PDPs were found across both the River Island 4 discharge face ($n = 10$, PDP21-30) and

the River Island 5 seepage face ($n = 10$, PDP31-40). PDP21 was dropped from further analysis as there were multiple clear periods of shallow temperature sensor desaturation where the temperature record warmed substantially and abruptly in a manner not reflected in deeper or adjacent PDP temperature records. Temperature loggers at PDP23, 26, and 35 had discrete periods of apparent short-term sensor malfunction amounting to a few days or less over the 4.5 months of data collection, and these times were removed from the respective records before running the vertical discharge flux models.

The recursive estimation methods require an estimate of discharge process variance, a parameter related to expected system noise and true short-term discharge flux variability. As in the McAliley et al. (2022) study, we found that setting the process variance parameter values from 1×10^{-4} to 1×10^{-5} m/day for EKF models reduced model output noise and preserved real, abrupt changes in discharge flux. Smaller values of process variance tended to overly smooth the discharge flux patterns to show little change at multiweek timescales even during known variation in river flow. For all sites, we first utilized a process variance of 1×10^{-4} m/day, and then for 17 PDP sites reduced to 1×10^{-5} m/day when there were clear time periods of enhanced or biased model residuals, as described in more detail by Haynes et al. (2023). All EKF discharge flux results are summarized in Figures 4 (Alsop Meadows) and 5 (River Island).

3.2 | Shallow versus deep source groundwater metrics

Alsop Meadows PDPs were predominately classified as shallow or mixed and River Island was predominantly classified as deep source groundwater (Table 2). Using the 0.03 m/day diurnal discharge signal amplitude threshold, 16 PDPs were classified as having a predominantly shallow groundwater source, and all but two of those locations were located within the Alsop Meadows discharge faces. When evaluating the more qualitative metric, weekly running minimum and maximum temperatures collected at 11 cm depth, 17 locations were classified as shallow, using a difference threshold of greater than 6°C, and all but three of these were along Alsop Meadows discharge faces. The remaining Alsop PDPs were classified as 'inconclusive' or having a maximum-minimum difference of 3–6°C. Six River Island PDPs had running weekly minimum to maximum differences less than 3°C and were therefore inferred to have potential deep groundwater sources. No sites with pronounced diurnal discharge flux patterns were classified as deep groundwater sources using the maximum-minimum difference, but seven sites without pronounced diurnal patterns had maximum-minimum difference >6°C (Figure 6).

3.3 | Local versus regional source groundwater metrics

Although groundwater source characteristic combinations of deep/local and shallow/regional are plausible, for this study we focused on the agreement between shallow/local and deep/regional metrics, as shown in Figures 4 and 5 and listed in Table 2. Significant seasonal trends were identified for 15 PDPs, most notably for all the Alsop 3 PDPs, but for only one of the River Island PDPs (Table 2). Only 11 PDP locations had substantial discharge flux rate direction reversals, and those were all observed along Alsop Meadows discharge faces. Seven Alsop PDPs were inferred to have shallow/local groundwater sources based on the diurnal discharge rate and both local metrics. No classification of shallow/local source groundwaters was determined for the River Island PDPs (Figure 5). Two Alsop PDPs also showed agreement between deep groundwater inference and both regional metrics, located along discharge face Alsop 2 (Figure 4). In contrast, 16 of the 19 River Island PDPs had an agreement between deep/regional groundwater source metrics (Figure 5).

3.4 | Chloride, stable isotopes, and dissolved radon

Although Alsop Meadows seepage faces 1 and 2 were in close spatial proximity, Cl^- concentrations were substantially higher for Alsop 2 across all monthly sampling events, generally ranging from 75 to 150 ppm (Figure 7a). River Island PDPs also showed high Cl^- concentrations, varying more than two-fold across each face (i.e., ~20–220 ppm; Figure 7b). Using the SE determined for all sample data, each seepage face in this study was classified as having convergent groundwater sources based on Cl^- concentrations (Table 2). The stable water isotope lc-excess metric indicated the greatest variability between the PDPs of Alsop Meadows discharge faces 1 and 2. Consequently, each was classified as having convergent groundwater sources (Figure 7c). Alsop Meadows 3 and the River Island discharge faces were classified as having common groundwater sources based on no significant variation in the lc-excess metric (Figure 7d). Dissolved radon was substantially higher for seepage faces Alsop 1, Alsop 2, and River Island 4 compared to Alsop 3 and River Island 5. Additionally, River Island 4 showed the greatest variation across all PDPs, ranging from 237 to 479 pCi/L (Figure 7e,f).

4 | DISCUSSION

4.1 | Evapotranspiration influence on shallow discharge flux patterns

Application of the new EKF flux modelling approach to vertical temperature records collected directly at points of focused groundwater discharge yielded a novel characterization of daily oscillations in flux magnitude (Figure 3, Table 2). Similar to numerous observations of diurnal water level patterns observed in shallow wells adjacent to surface waters (e.g., Gribovszki et al., 2010; Harmon et al., 2020; Lautz, 2008; Rosenberry & Winter, 1997), we attribute these oscillations to the influence of ET processes on shallow source groundwater flowpaths. Daily streamflow patterns have also often been recorded during summer and attributed to riparian and hillslope scale

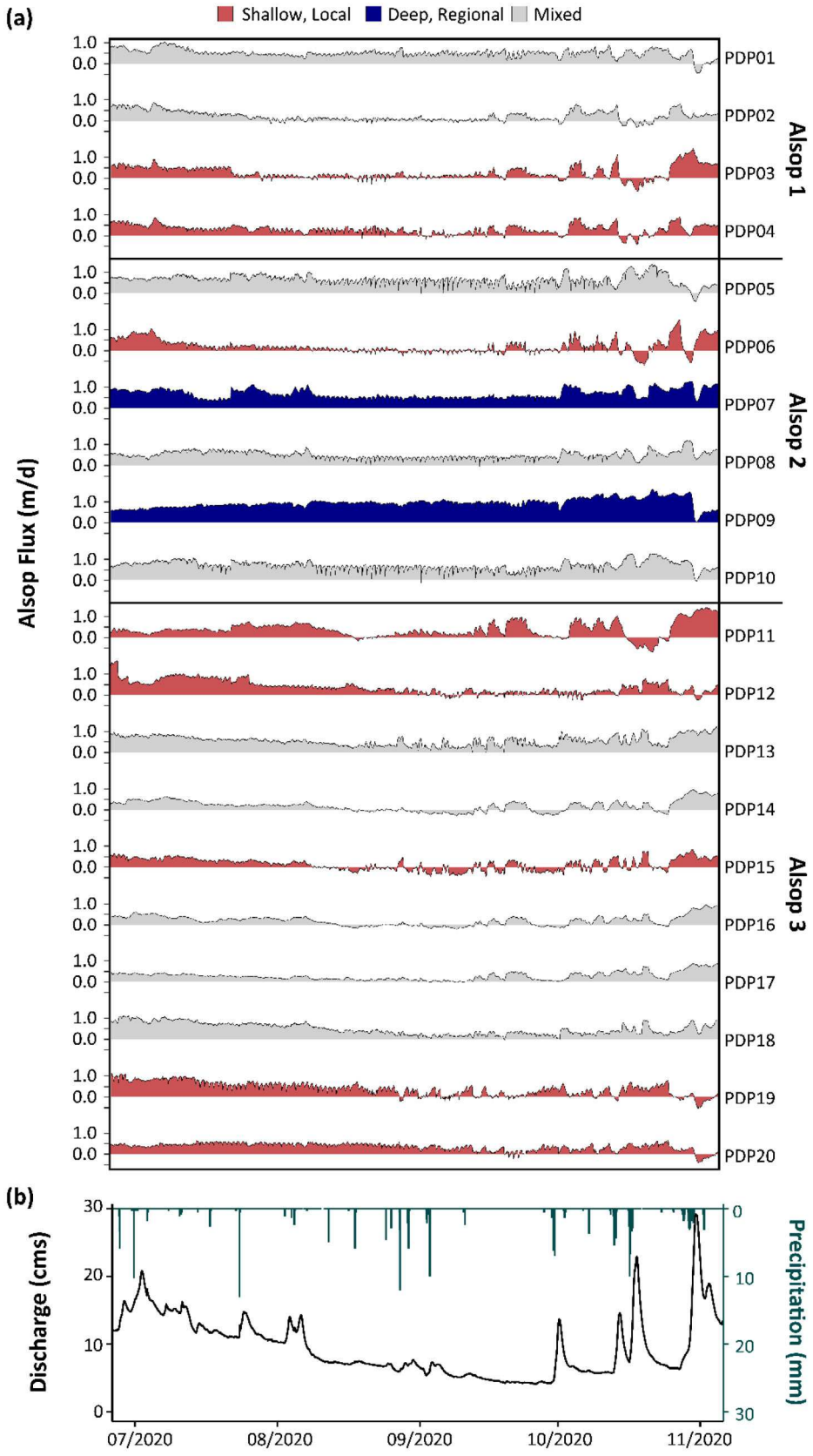

FIGURE 4 (a) Displays all Alsop Meadows preferential discharge point (PDP) discharge flux patterns derived with the extended Kalman Filter (EKF) model (no 95% CI) and sites classified as being shallow/local (red) or deep/regional (blue) or mixed signal (grey) groundwater sources. Discharge (upward flow direction) is indicated by positive values for ease of interpretation. A mixed source (or inconclusive) groundwater characterization was defined when either shallow/local or deep/regional metrics did not agree. Site numbers are displayed on the right *y*-axis with respective PDP discharge faces. (b) Shows the Farmington River streamflow (USGS site no. 01189995) and local precipitation record for the measurement period (U.S. Geological Survey, 2023).

ET (e.g., Gribovszki et al., 2010; Lundquist & Cayan, 2002), though direct measurement of diel discharge fluxes has only been demonstrated a small number of times, using instrumentation deployed below the waterline (Rosenberry et al., 2013). ET-influenced discharge flux patterns have not yet been quantified in detail (e.g., Figure 6) along exposed riverbank discharges (to our

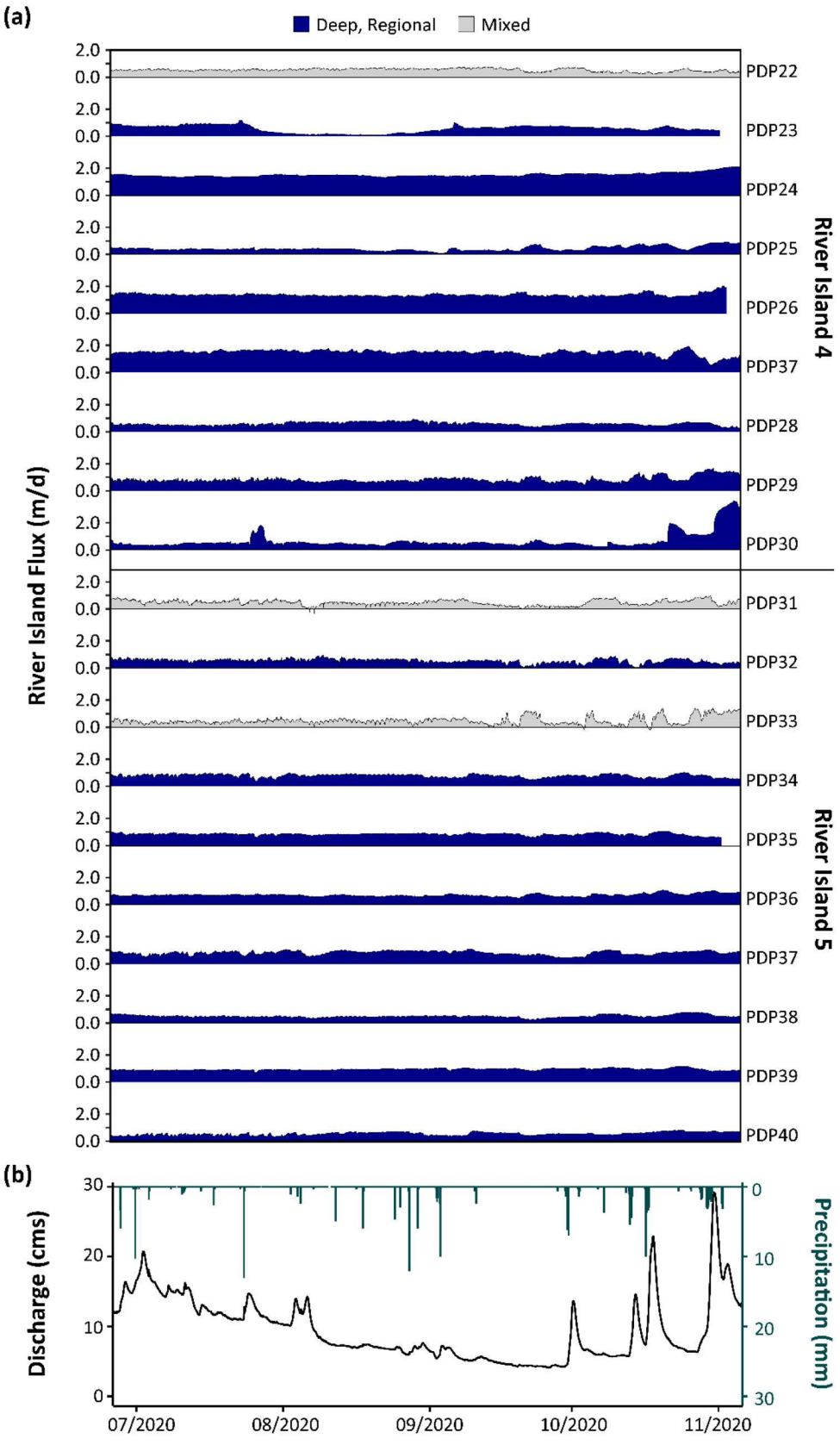

FIGURE 5 (a) Displays all River Island preferential discharge point (PDP) discharge flux patterns derived with the extended Kalman Filter (EKF) model (no 95% CI) and sites classified as being deep/regional (blue) or mixed (grey) groundwater sources. Discharge (upward flow direction) is indicated by positive values for ease of interpretation. A mixed source (or inconclusive) groundwater characterization was defined when either shallow/local or deep/regional metrics did not agree. Site numbers are displayed on the right y-axis with respective PDP discharge faces. (b) Shows the Farmington River streamflow (USGS site no. 01189995) and local precipitation record for the measurement period (U.S. Geological Survey, 2023).

knowledge), and the recently developed EKF vertical temperature profiler analysis method was key to that advance. Lautz (2012) applied more commonly used analytical vertical temperature analysis methods of Gordon et al. (2012) to data collected along a beaver-influenced Wyoming stream that indicated diurnal discharge flux pumping was occurring during discrete multiday periods. However,

TABLE 2 Interpreted source groundwater flowpath metrics for all preferential discharge point locations (metrics are described in Table 1) with the average diurnal discharge flux pattern amplitude listed in parenthesis under the 'diurnal discharge' column.

		Shallow versus deep flowpath		Local versus regional flowpath		Common versus convergent	
Discharge face	PDP	Diurnal discharge pattern (m/day)	Max–min temperature diff.	Seasonal discharge pattern	Riverbank storage	Chloride concentration	Lc-excess
Alsop 1	PDP01	Shallow (0.04)	Shallow	Regional	Local	Convergent	Convergent
	PDP02	Shallow (0.03)	Shallow	Local	Regional		
	PDP03	Shallow (0.04)	Shallow	Local	Local		
	PDP04	Shallow (0.04)	Shallow	Local	Local		
Alsop 2	PDP05	Shallow (0.06)	Inconclusive	Regional	Local	Convergent	Convergent
	PDP06	Shallow (0.05)	Inconclusive	Local	Local		
	PDP07	Deep (0.02)	Inconclusive	Regional	Regional		
	PDP08	Shallow (0.03)	Inconclusive	Regional	Regional		
	PDP09	Deep (0.01)	Inconclusive	Regional	Regional		
	PDP10	Shallow (0.06)	Inconclusive	Regional	Regional		
Alsop 3	PDP11	Shallow (0.03)	Shallow	Local	Local	Convergent	Common
	PDP12	Shallow (0.04)	Shallow	Local	Local		
	PDP13	Shallow (0.04)	Shallow	Local	Regional		
	PDP14	Deep (0.02)	Shallow	Local	Local		
	PDP15	Shallow (0.05)	Shallow	Local	Local		
	PDP16	Deep (0.01)	Shallow	Local	Regional		
	PDP17	Deep (0.02)	Shallow	Local	Regional		
	PDP18	Deep (0.02)	Shallow	Local	Regional		
	PDP19	Shallow (0.05)	Shallow	Local	Local		
	PDP20	Shallow (0.03)	Shallow	Local	Local		
River Island 4	PDP22	Shallow (0.03)	Inconclusive	Regional	Regional	Convergent	Common
	PDP23	Deep (0.01)	Deep	Regional	Regional		
	PDP24	Deep (0.00)	Deep	Regional	Regional		
	PDP25	Deep (0.01)	Inconclusive	Regional	Regional		
	PDP26	Deep (0.01)	Deep	Regional	Regional		
	PDP27	Deep (0.01)	Deep	Regional	Regional		
	PDP28	Deep (0.02)	Inconclusive	Regional	Regional		
	PDP29	Deep (0.02)	Deep	Regional	Regional		
	PDP30	Deep (0.01)	Inconclusive	Regional	Regional		
River Island 5	PDP31	Deep (0.02)	Shallow	Local	Regional	Convergent	Common
	PDP32	Deep (0.02)	Shallow	Regional	Regional		
	PDP33	Shallow (0.06)	Inconclusive	Regional	Regional		
	PDP34	Deep (0.02)	Inconclusive	Regional	Regional		
	PDP35	Deep (0.00)	Inconclusive	Regional	Regional		
	PDP36	Deep (0.01)	Deep	Regional	Regional		
	PDP37	Deep (0.01)	Inconclusive	Regional	Regional		
	PDP38	Deep (0.02)	Inconclusive	Regional	Regional		
	PDP39	Deep (0.01)	Inconclusive	Regional	Regional		
	PDP40	Deep (0.01)	Shallow	Regional	Regional		

the interpretation of those apparent subdaily discharge patterns was uncertain as they were characterized using analytical models based on daily temperature signals.

Through initial testing for this study, we also found it difficult to quantify diurnal flux patterns with confidence using the VFLUX software methods (Haynes et al., 2023). It can also be challenging to

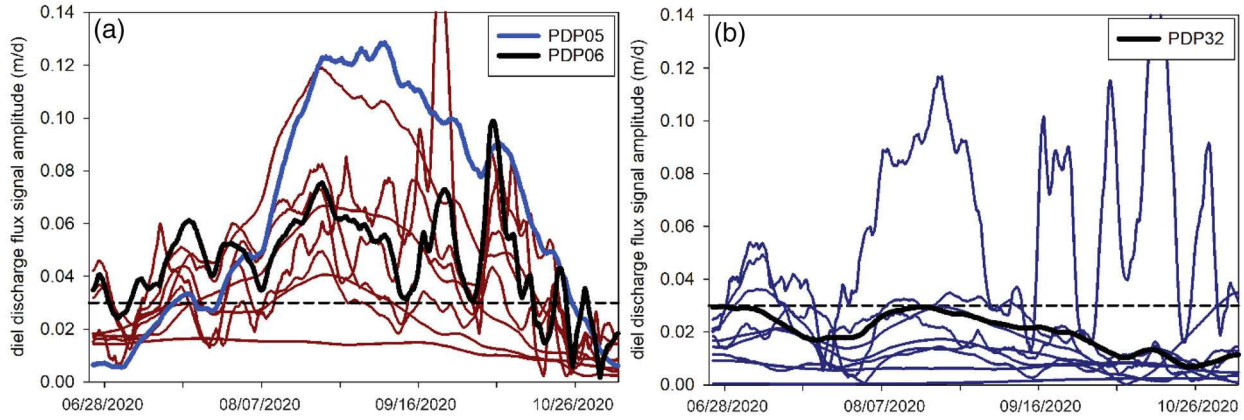

FIGURE 6 Extracted diurnal discharge flux signal amplitudes are shown for all preferential discharge point (PDP) locations across the (a) Alsop 1 and 2, and (b) River Island 5 discharge faces. Specific PDPs shown in detail in Figure 3 are highlighted with thicker lines as indicated by the panel legends.

disentangle source flowpath-scale ET influence on submerged discharge points as variation in daily streamflow magnitude and velocity impact pressure along the riverbed, influencing discharge flux rates. By collecting vertical temperature data directly in exposed riverbank discharges and modelling subdaily discharge flux patterns with the EKF method, we have more confidently captured the variable influence of ET on source groundwaters to individual discharge points. These findings highlight new research opportunities that more directly pair diurnal discharge fluxes with evaluations of stream corridor ET to better understand the environmental drivers of the patterns described in Figure 6. In late summer at several of our study sites, the relative magnitude in ET-driven diurnal flux variation observed in this study of large riverbank discharge faces generally exceeded the 10% diel variability previously recorded along a lakebed using automated seepage meter, at times effectively shutting down PDPs during the afternoons (Figure 3a,b).

Through a combination of stream and well pressure measurements, Harmon et al. (2020) found that ET signals in near-stream shallow groundwater varied in space due in part to geologic heterogeneity. They also observed the amplitude of diurnal stream stage fluctuations to generally peak in late summer while shorter term groundwater fluctuations were related to soil water storage (increased ET signals) and cloud/smoke cover (decreased ET signals). We found a similar August through September peak in diurnal pumping for Alsop Meadows sites that exceeded our shallow groundwater classification signal amplitude threshold of 0.03 m/day (Figure 6a). Also observed were abrupt short-term changes in diurnal discharge flux amplitude that may be tied to the combination of air temperature and soil moisture. However, further analysis of the specific ET controls is beyond the scope of the current study. In addition to transpiration, Alsop Meadows discharge faces are directly adjacent to irrigated lands (i.e., golf course) and shallow floodplain wetlands and ponds (Figure 1), which may further complicate the net ET signal. Most of the River Island PDPs that we inferred to show deeper and more regional source groundwater characteristics showed little diurnal fluctuation (Figure 6b), indicating deeper source flowpaths not directly accessed by plants and ponds. The EKF advance in subdaily discharge flux monitoring addresses research priorities put forth by Singha and Navarre-Sitchler (2021) and may help diagnose the vulnerability of stream aquatic habitats as ET fluxes generally increase in the northeastern United States under a warming climate, drawing down shallow groundwater (Condon et al., 2020).

4.2 | Seasonal discharge patterns and flux reversals

Shallow groundwater sourced PDPs are expected to be sensitive to long-term climate warming and shorter-term precipitation patterns (Kurylyk et al., 2014). We found that 15 out of 39 PDPs that were monitored in detail for this study effectively shut down as PDPs during mid- to late-summer in 2020. This observed seasonality in major riverbank discharge has interesting implications. At local scales, if shallow groundwater-sourced discharge faces are reduced during dry times, associated cold-water patches in the adjacent channel would also be minimized. Reduction of relatively cold water inflows to warm rivers in summer likely reduces the potential for shallow groundwater-sourced PDPs to create thermal refuges, as the distribution of cold water fish in such patches has been shown to be highly sensitive to flow rate and thermal mixing (Morgan & O'Sullivan, 2022). Seasonal patterns of shallow groundwater discharge may also explain why shallow groundwater dominated streams generally show reduced baseflow scores compared to deep groundwater dominated streams, nationally (Hare et al., 2021). Alsop Meadows 3 is an example of a major riverbank discharge feature with persistent seasonal reductions in discharge rate (all 10 monitored PDPs), and the other Alsop faces showed a more mixed response to seasonal drydown. In contrast, the River Island sites had only one PDP out of 19 where a strong seasonal pattern was observed, with flux rates generally greater than >1 md^{-1}, yielding a

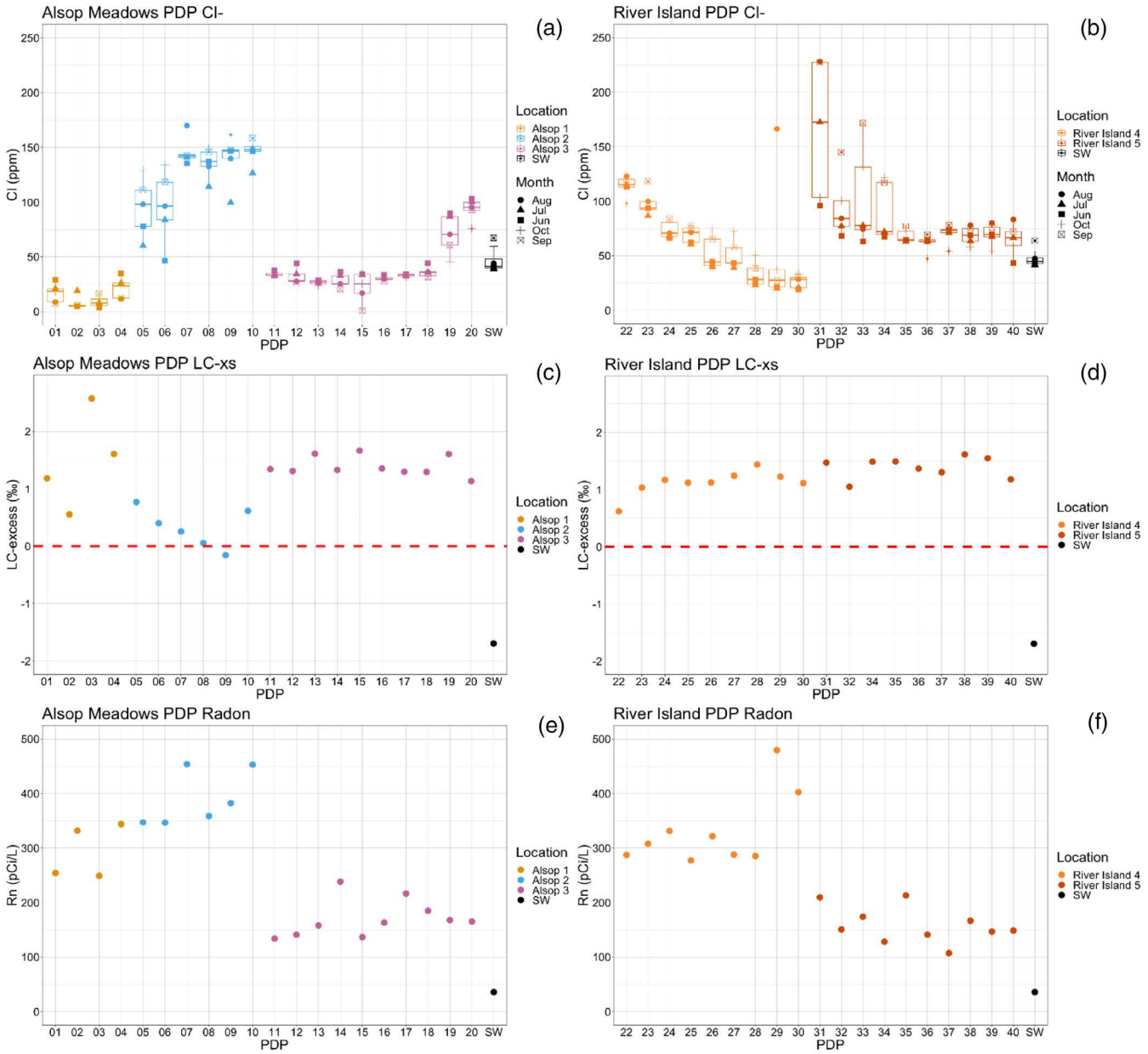

FIGURE 7 Temporal Cl^- data collected across (a) Alsop Meadows and (b) River Island discharge faces, respectively. (c, d) lc-excess from a single stable water isotope sampling event, and (e, f) dissolved radon gas concentration collected at the same time. In (a) and (b) the seasonal means and quartiles of Cl^- concentrations are shown as box plots, and the remaining plots show the results of one spatial sampling event.

more consistent source of baseflow to the mainstem river system sourced by deep/regional groundwater.

During high river flow events, riverbank storage can enhance river corridor denitrification by pulsing electron donors and acceptors into reactive bank sediments and enhancing mixing (Shuai et al., 2019). As river stage drops, the release of water from bank storage can then supply river flow, extending the influence of individual precipitation events (Rhodes et al., 2017). Unlike many mainstem rivers, the Farmington River is not significantly impacted by major dam releases and bank storage events are most likely to be caused by melt and storm flows. Over the summer to fall monitoring period of 2020, we found that 11 of the Alsop Meadow PDPs experienced at least one full day of discharge flux reversal, yet none of the River Island flux records met that criterion (Figures 4 and 5). Although river flow during the late season events was of a similar high magnitude to flows early in the summer, apparent exchanges of river water into riverbank sediments were not observed for any locations early in the sampling period. These observations highlight the seasonal control of river floodplain groundwater head, even for locally sourced groundwaters. Following the fundamental principles of Darcy's Law, as water table elevations fall over the summer, local (shorter) flowpaths are expected to show greater discharge flux variability as impacted by river stage compared to regional (longer) flowpaths, where the lateral hydraulic gradient is dominated by flowpath length (Briggs et al., 2018). This physical

mechanism explains why many of the Alsop Meadows PDPs that showed pronounced ET influence and seasonal discharge reduction also tended to have late season discharge flux reversals (Figure 4) in contrast to the more stable discharge patterns observed at the River Island sites (Figure 5).

4.3 | Groundwater discharge constituent characterization

Constituents and tracers measured in water samples from PDP discharge locations indicated variations in concentrations, both among the Farmington River discharge faces and within them. Although located in close physical proximity, Alsop Meadows discharge faces 1 and 2 had contrasting Cl^- profiles, whereas Alsop 2 had substantially higher and more temporally variable Cl^- concentrations generally ranging from 100 to 150 mg/L (Figure 7). Alsop 2 also had more heterogeneous discharge flux patterns and may show greater local influence from shallow floodplain ponds (evaporative Cl^- concentration) and anthropogenic (road salting, irrigation) Cl^- sources.

The River Island discharge faces showed strong spatial gradients in Cl^- concentration that persisted over the study period, even though the discharge flux patterns indicated a dominance of deep/regional source groundwater (Figure 5, Table 2). We attribute the observed chemical variability to variability in discrete Cl^- sources local to the discharge faces. All PDP locations had roads, active agriculture, or golf course turf within 200 m of the riverbank, which are all possible Cl^- sources (Gutchess et al., 2016) and may imprint on regional groundwater sources proximal to discharge via vertical percolation. Given the conservative nature of Cl^- transport in groundwater, riparian buffers do little to mitigate Cl^- along river corridors, and our study indicates substantial fine-grained spatial discharge characterization may be necessary to estimate Cl^- loading to rivers from preferential groundwater discharges.

The isotopic lc-excess metric showed less variability among and within the study discharge faces, and only Alsop Meadows faces 1 and 2 showed enough inter PDP variation to indicate distinct groundwater sources. Although the differences are subtle, lc-excess patterns at those sites may reflect evaporation processes from proximal floodplain ponds, features not found immediately upgradient of the other study discharge faces. This supports the general characterization of shallow/local groundwater sources and potential contribution of pond surface evaporation to the observed diurnal discharge pumping patterns. Fundamentally, lc-excess is only useful in parsing various source groundwater flowpaths when a subset has experienced pronounced evaporation typical of exchange with surface water features. Although we did not use ^{222}Rn to classify the PDPs as indicated in Table 2, observed concentrations were highest across discharge faces Alsop 1 and 2, and River Island 4. We did not anticipate high concentrations at the Alsop sites, as we expected higher concentrations of radon to be related to bedrock sources. Instead, the high concentrations observed at the Alsop sites with deep bedrock likely indicate ^{222}Rn production in the unconsolidated valley sediments. As detailed by Schaper et al. (2022), radon production can be highly variable at local scales within alluvial material, complicating the use as a quantitative tracer of groundwater sources and travel times.

4.4 | Common versus convergent source groundwater conceptual models and geologic controls

The dichotomy of common and convergent conceptualizations has limitations in terms of capturing the potential variety of groundwater expression along mainstem riverbanks. Our results show that discharge faces express varying degrees of converging groundwater flowpaths. Discharge faces can have common general source depths and lengths but also have groundwater chemistry that indicates distinct sources that converge at the discharge face (i.e., Alsop 1). We believe that is a function of how groundwater flowpaths integrate multiscale chemical legacies and may show discharge concentrations that are influenced by immediate river corridor sources. In this case, variable Cl^- application to anthropogenic features near the river likely influenced both shallow/local and deep/regional discharge concentrations. Given the multiscale complexity in groundwater chemistry, the toolkit elements presented here based on physical flux patterns may be more reliable for inference of general source groundwater characteristics.

The dominance of apparent deep/regional groundwater sources to the River Island PDPs may be explained by the underlying bedrock geology of those sites relative to Alsop Meadows. On average, the bedrock contact under the River Island discharge faces was 40% shallower than the Alsop faces. Along the River Island reach the river flows normal to the dipping bedrock strike, a situation thought to enhance groundwater discharge, especially from sedimentary bedding. When the upper 32 m of the streambed electrical resistivity geophysical imaging of the White et al. (2020) dataset are plotted along the reach, clusters of mapped PDPs generally coincide with other major resistive streambed features and occur along opposing banks (Figure 8). Those resistive features have previously been interpreted as dipping sandstone bedrock units (Lane et al., 2020). Water-bearing sandstone bedrock units cutting perpendicularly across the riverbed provides a mechanistic explanation for the deep/regional discharge flux patterns that dominated the River Island discharge faces. The implications of riverbank discharge from deep/regional sources to legacy contaminant transport are profound. For example, pilot scale PFAS compound sampling at a subset of the PDPs found older and more toxic compounds associated with the River Island groundwater discharge (Baranovic, 2022).

5 | CONCLUSIONS

Groundwater discharge source characteristics influence a wide range of ecological and environmental patterns and processes, from

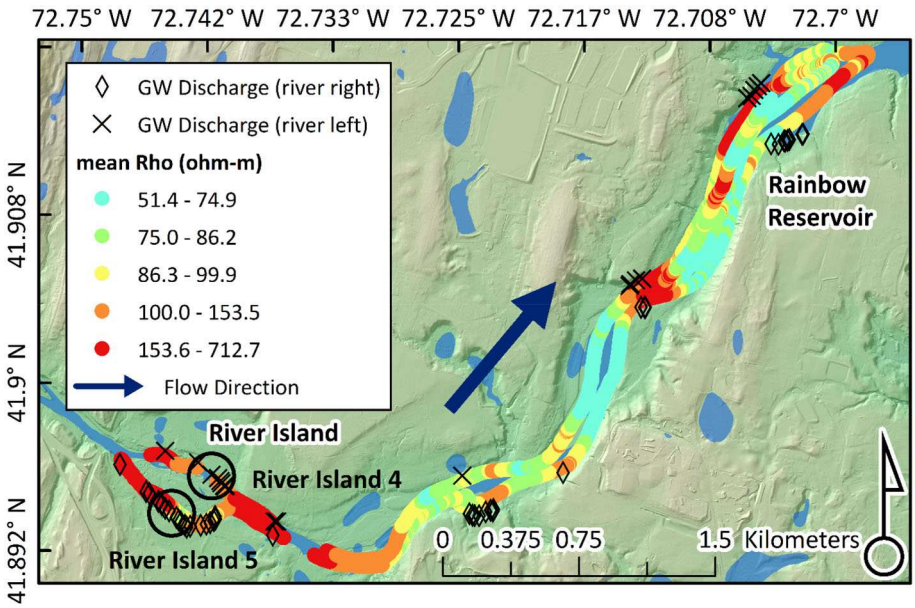

FIGURE 8 A comparison of mean streambed electrical resistivity calculated over 0–32 m riverbed depths based on transient electromagnetic imaging (White et al., 2020). Zones of high bedrock electrical resistivity are interpreted as permeable dipping sandstone units that cut across the river channel and provide groundwater pathways to the River Island and other discharge faces mapped with thermal infrared (TIR). Map layers in the form of hillshade rasters and DEMs were derived from Connecticut Lidar Data downloaded from the Connecticut Department of Energy and Environmental Protection (CT ECO, 2016) and stream networks are provided by Barclay et al. (2020).

landscape-scale legacy contaminant transport (Ransom et al., 2022), to niche cold water habitat (Sullivan et al., 2021), baseflow regimes (Hare et al., 2021), and near-stream biogeochemical processes (Hester & Fox, 2020). Using common watershed scale groundwater flow modelling techniques, Barclay et al. (2020) found that fundamental source groundwater characteristics along the Farmington River were uncertain, as models with similar calibration metrics predicted disparate attributes related to source flowpath depth (e.g., deep vs. shallow) and length (e.g., local vs. regional). That uncertainty is strongly influenced by underinformed geologic structure, even in the Farmington River watershed where soils and bedrock maps are augmented by recent geophysical data collection. By efficiently identifying PDPs in the field using TIR, and monitoring temporal discharge flux rate patterns and constituents, groundwater sources can be inferred providing additional data with which to evaluate model predictions. Here we describe, implement, and evaluate an approach for assessing multiscale temporal discharge flux attributes over five extensive riverbank discharge faces to assess whether discharge faces represented common or convergent source groundwater flowpaths. Practically, if discharge faces along mainstem rivers tend to be dominated by common groundwater sources, sampling strategies can remain simplified to a few representative PDPs for the assessment of legacy contaminant transport and other management relevant characteristics as described by Barclay et al. (2020). However, if discharge faces do indeed represent a focused convergence of a wide range of flowpath depths, lengths, and ages, numerous PDPs need to be evaluated across each discharge face to assess source groundwater characteristics.

Given the outsized influence major groundwater discharges can have on localized aquatic habitat and larger river ecosystem dynamics (i.e., control points), it is important that we explicitly evaluate the groundwater flowpaths contributing to extensive discharge faces. Such understanding influences a range of management relevant groundwater discharge characteristics, including vulnerability to drought, climate change, and legacy contaminant transport. Along the Farmington River, we found support for a modified conceptual model of groundwater flowpath convergence along the riverbank. The upstream Alsop Meadows discharge faces that occurred over thick valley sediments indicated the greatest density of shallow/local groundwater sources. The downstream River Island sites that occurred over thinner sediments and known permeable bedrock features intersecting the river corridor were dominated by deep/regional source groundwater indicators. Our study highlights the importance of combining multiple source groundwater inference metrics and the utility of new discharge flux modelling approaches in capturing multiscale temporal patterns that are diagnostic of a range of physical processes relevant to river corridor science and management.

ACKNOWLEDGEMENTS

The work by Adam Haynes was done while serving as a graduate student contractor with the U.S. Geological Survey. We acknowledge field and laboratory help from Fiona Liu, Lauren Koenig, Kenneth Bell, and Huayile Zhang. This research was funded by U.S. National Science Foundation Division of Earth Sciences award (#1824820) and the U.S. Geological Survey (USGS) Toxic Substances Hydrology Program. Data used for this study are publicly available as detailed in the reference list (Haynes et al., 2023; Jackson et al., 2023; Moore, Haynes, et al., 2023; Moore, Jackson, et al., 2023; White et al., 2020). Any use of trade, firm, or product names is for descriptive purposes only and does not imply endorsement by the U.S. Government.

DATA AVAILABILITY STATEMENT

The data that support the findings of this study are openly available in from the U.S. Geological Survey ScienceBase repository (https://www.sciencebase.gov/catalog/) as detailed in the reference list.

ORCID

Adam B. Haynes https://orcid.org/0000-0002-0190-2976
Martin A. Briggs https://orcid.org/0000-0003-3206-4132
Eric Moore https://orcid.org/0000-0002-2479-2677
Kevin Jackson https://orcid.org/0000-0002-2156-5073
James Knighton https://orcid.org/0000-0002-4162-996X
David M. Rey https://orcid.org/0000-0003-2629-365X
Ashley M. Helton https://orcid.org/0000-0001-6928-2104

REFERENCES

Baranovic, A. (2022). *Investigating PFAS patterns in aquatic ecosystems* (master's thesis). University of Connecticut.

Barclay, J. R., Briggs, M. A., Moore, E. M., Starn, J. J., Hanson, A. E. H., & Helton, A. M. (2022). Where groundwater seeps: Evaluating modeled groundwater discharge patterns with thermal infrared surveys at the river-network scale. *Advances in Water Resources*, *160*, 104108. https://doi.org/10.1016/j.advwatres.2021.104108

Barclay, J. R., Starn, J. J., Briggs, M. A., & Helton, A. M. (2020). Improved prediction of management-relevant groundwater discharge characteristics throughout river networks. *Water Resources Research*, *56*. https://doi.org/10.1029/2020WR028027

Basu, N. B., Van Meter, K. J., Byrnes, D. K., Van Cappellen, P., Brouwer, R., Jacobsen, B. H., Jarsjö, J., Rudolph, D. L., Cunha, M. C., Nelson, N., Bhattacharya, R., Destouni, G., & Olsen, S. B. (2022). Managing nitrogen legacies to accelerate water quality improvement. *Nature Geoscience*, *15*, 97–105. https://doi.org/10.1038/s41561-021-00889-9

Boano, F., Demaria, A., Revelli, R., & Ridolfi, L. (2010). Biogeochemical zonation due to intrameander hyporheic flow. *Water Resources Research*, *46*, W02511. https://doi.org/10.1029/2008wr007583

Bourke, S. A., Cook, P. G., Shanafield, M., Dogramaci, S., & Clark, J. F. (2014). Characterisation of hyporheic exchange in a losing stream using radon-222. *Journal of Hydrology*, *519*, 94–105. https://doi.org/10.1016/j.jhydrol.2014.06.057

Briggs, M. A., & Hare, D. K. (2018). Explicit consideration of preferential groundwater discharges as surface water ecosystem control points. *Hydrological Processes*, *32*, 2435–2440. https://doi.org/10.1002/hyp.13178

Briggs, M. A., Harvey, J. W., Hurley, S. T., Rosenberry, D. O., McCobb, T., Werkema, D., & Lane, J. W., Jr. (2018). Hydrogeochemical controls on brook trout spawning habitats in a coastal stream. *Hydrology and Earth System Sciences*, *6383–6398*, 6383–6398. https://doi.org/10.5194/hess-22-6383-2018

Briggs, M. A., Jackson, K. E., Liu, F., Moore, E. M., Bisson, A., & Helton, A. M. (2022). Exploring local riverbank sediment controls on the occurrence of preferential groundwater discharge points. *Water*, *14*. https://doi.org/10.3390/w14010011

Briggs, M. A., Lautz, L. K., Buckley, S. F., & Lane, J. W. (2014). Practical limitations on the use of diurnal temperature signals to quantify groundwater upwelling. *Journal of Hydrology*, *519*, 1739–1751. https://doi.org/10.1016/j.jhydrol.2014.09.030

Briggs, M. A., Tokranov, A. K., Hull, R. B., LeBlanc, D. R., Haynes, A. B., & Lane, J. W. (2020). Hillslope groundwater discharges provide localized stream ecosystem buffers from regional per- and polyfluoroalkyl substances (PFAS) contamination. *Hydrological Processes*, *34*, 2281–2291. https://doi.org/10.1002/hyp.13752

Brookfield, A. E., Hansen, A. T., Sullivan, P. L., Czuba, J. A., Kirk, M. F., Li, L., Newcomer, M. E., & Wilkinson, G. (2021). Predicting algal blooms: Are we overlooking groundwater? *Science of the Total Environment*, *769*, 144442. https://doi.org/10.1016/j.scitotenv.2020.144442

Burns, D. A., Murdoch, P. S., Lawrence, G. B., & Michel, R. L. (1998). Effect of groundwater springs on NO, concentrations during summer in Catskill Mountain streams. *Water Resources Research*, *34*, 1987–1996.

Cassanelli, J. P., & Robbins, G. A. (2013). Effects of road salt on Connecticut's groundwater: A statewide centennial perspective. *Journal of Environmental Quality*, *42*, 737–748.

Condon, L. E., Atchley, A. L., & Maxwell, R. M. (2020). Evapotranspiration depletes groundwater under warming over the contiguous United States. *Nature Communications*, *11*, 873. https://doi.org/10.1038/s41467-020-14688-0

Constantz, J. (2008). Heat as a tracer to determine streambed water exchanges. *Water Resources Research*, *44*, W00d10. https://doi.org/10.1029/2008wr006996

CT Eco. (2016). *Connecticut Statewide LiDAR*, 2016. https://cteco.uconn.edu/data/download/flight2016/index.htm

Eggleston, J., & McCoy, K. J. (2015). Assessing the magnitude and timing of anthropogenic warming of a shallow aquifer: Example from Virginia Beach, USA. *Hydrogeology Journal*, *23*, 105–120. https://doi.org/10.1007/s10040-014-1189-y

Gordon, R. P., Lautz, L. K., Briggs, M. A., & McKenzie, J. M. (2012). Automated calculation of vertical pore-water flux from field temperature time series using the VFLUX method and computer program. *Journal of Hydrology*, *420–421*, 142–158. https://doi.org/10.1016/j.jhydrol.2011.11.053

Gribovszki, Z., Szilágyi, J., & Kalicz, P. (2010). Diurnal fluctuations in shallow groundwater levels and streamflow rates and their interpretation——A review. *Journal of Hydrology*, *385*, 371–383. https://doi.org/10.1016/j.jhydrol.2010.02.001

Gutchess, K., Jin, L., Lautz, L., Shaw, S. B., Zhou, X., & Lu, Z. (2016). Chloride sources in urban and rural headwater catchments, central New York. *Science of the Total Environment*, *565*, 462–472. https://doi.org/10.1016/j.scitotenv.2016.04.181

Handcock, R. N., Torgersen, C. E., Cherkauer, K. A., Gillespie, A. R., Tockner, K., Faux, R. N., & Tan, J. (2012). Thermal infrared remote sensing of water temperature in riverine landscapes. In *Fluvial remote sensing for science and management* (pp. 85–113). John Wiley & Sons Inc.

Hare, D. K., Helton, A. M., Johnson, Z. C., Lane, J. W., & Briggs, M. A. (2021). Continental-scale analysis of shallow and deep groundwater contributions to streams. *Nature Communications*, *12*, 1450. https://doi.org/10.1038/s41467-021-21651-0

Harmon, R., Barnard, H. R., & Singha, K. (2020). Water table depth and bedrock permeability control magnitude and timing of transpiration-induced diel fluctuations in groundwater. *Water Resources Research*, *56*, 1–22. https://doi.org/10.1029/2019WR025967

Haynes, A. B., Briggs, M. A., Moore, E., Rey, D. M., Jackson, K. E., & Helton, A. M. (2023). *Riverbank vertical temperature profiler data and calculated groundwater discharge flux estimates from the Farmington River corridor, CT, USA*. U.S. Geological Survey Public Data Base Release. https://doi.org/10.5066/P9B3CYWW

Hester, E. T., & Fox, G. A. (2020). Preferential Flow in riparian groundwater: Gateways for watershed solute transport and implications for water quality management. *Water Resources Research*, *56*, 1–8. https://doi.org/10.1029/2020WR028186

Hoehn, E., & von Gunten, H. R. (1989). Radon in groundwater: a tool to assess infiltration from surface waters to aquifers. *Water Resources Research*, *25*, 1795–1803.

Irvine, D. J., Lautz, L. K., Briggs, M. A., Gordon, R. P., & Mckenzie, J. M. (2015). Experimental evaluation of the applicability of phase, amplitude, and combined methods to determine water flux and thermal diffusivity from temperature time series using VFLUX 2. *Journal of Hydrology*, *531*, 728–737. https://doi.org/10.1016/j.jhydrol.2015.10.054

Jackson, K. E., Haynes, A. B., & Briggs, M. A. (2023). *Passive seismic depth to bedrock data collected along streams of the Farmington River watershed, CT, USA*. U.S. Geological Survey Data Release. https://doi.org/10.5066/P9FTZ0DK

Kampen, R., Schneidewind, U., Anibas, C., Bertagnoli, A., Tonina, D., Vandersteen, G., Luce, C., Krause, S., & Berkel, M. (2022). LPMLE

n——A frequency domain method to estimate vertical streambed fluxes and sediment thermal properties in semi-infinite and bounded domains. *Water Resources Research*, *58*, 1–13. https://doi.org/10.1029/2021wr030886

Kang, X., Shi, X., Deng, Y., Revil, A., Xu, H., & Wu, J. (2018). Coupled hydrogeophysical inversion of DNAPL source zone architecture and permeability field in a 3D heterogeneous sandbox by assimilation time-lapse cross-borehole electrical resistivity data via ensemble Kalman filtering. *Journal of Hydrology*, *567*, 149–164. https://doi.org/10.1016/j.jhydrol.2018.10.019

Knighton, J. (2021). *Fenton tract research forest——Hydrologic data*. HydroShare.

Kurylyk, B. L., MacQuarrie, K. T. B., & McKenzie, J. M. (2014). Climate change impacts on groundwater and soil temperatures in cold and temperate regions: Implications, mathematical theory, and emerging simulation tools. *Earth-Science Reviews*, *138*, 313–334. https://doi.org/10.1016/j.earscirev.2014.06.006

Lane, J. W., Briggs, M. A., Maurya, P. K., White, E. A., Pedersen, J. B., Auken, E., Terry, N., Minsley, B., Kress, W., LeBlanc, D. R., Adams, R., & Johnson, C. D. (2020). Characterizing the diverse hydrogeology underlying rivers and estuaries using new floating transient electromagnetic methodology. *Science of the Total Environment*, *740*, 140074. https://doi.org/10.1016/j.scitotenv.2020.140074

Lautz, L. K. (2008). Estimating groundwater evapotranspiration rates using diurnal water table fluctuations in a semi-arid riparian zone. *Hydrogeology Journal*, *16*, 483–497.

Lautz, L. K. (2012). Observing temporal patterns of vertical flux through streambed sediments using time-series analysis of temperature records. *Journal of Hydrology*, *464–465*, 199–215. https://doi.org/10.1016/j.jhydrol.2012.07.006

Leach, J. A., Kelleher, C., Kurylyk, B. L., & dan Moore, R. (2022). A primer on stream temperature processes. *WIREs Water*, *1–18*. https://doi.org/10.1002/wat2.1643

LeRoux, N. K., Kurylyk, B. L., Briggs, M. A., Irvine, D. J., Tamborski, J. J., & Bense, V. F. (2021). Using heat to trace vertical water fluxes in sediment experiencing concurrent tidal pumping and groundwater discharge. *Water Resources Research*, *57*, 1–13. https://doi.org/10.1029/2020WR027904

Luce, C. H., Tonina, D., Gariglio, F., & Applebee, R. (2013). Solutions for the diurnally forced advection-diffusion equation to estimate bulk fluid velocity and diffusivity in streambeds from temperature time series. *Water Resources Research*, *49*, 488–506. https://doi.org/10.1029/2012WR012380

Lundquist, J. D., & Cayan, D. R. (2002). Seasonal and spatial patterns in diurnal cycles in streamflow in the western United States. *Journal of Hydrometeorology*, *3*, 591–603. https://doi.org/10.1175/1525-7541(2002)003<0591:SASPID>2.0.CO;2

Marcelli, M. F., Burns, E. R., Muffler, L. J. P., Meigs, A., Curtis, J. A., & Torgersen, C. E. (2022). Effects of structure and volcanic stratigraphy on groundwater and surface water flow: Hat Creek basin, California, USA. *Hydrogeology Journal*, *31*, 219–240. https://doi.org/10.1007/s10040-022-02545-x

McAliley, W. A., Day-Lewis, F. D., Rey, D., Briggs, M. A., Shapiro, A. M., & Werkema, D. (2022). Application of recursive estimation to heat tracing for groundwater/surface-water exchange. *Water Resources Research*, *58*, 1–18. https://doi.org/10.1029/2021wr030443

Modica, E. (1999). *Source and age of ground-water seepage to streams* (USGS Fact Sheet 063-99).

Moore, E. M., Haynes, A. B., Jackson, K. E., Bisson, A. M., Barclay, J. R., Liu, F., Briggs, M. A., & Helton, A. (2023). *Biogeochemical and source characteristics of preferential groundwater discharge in the Farmington River watershed (Connecticut and Massachusetts, 2017–2021)*. U.S. Geological Survey Data Release. https://doi.org/10.5066/P941XKST

Moore, E. M., Jackson, K. E., Haynes, A. B., Harvey, M., Helton, A. M., & Briggs, M. A. (2023). *Thermal infrared images of groundwater discharge zones in the Farmington and Housatonic River watersheds (Connecticut and Massachusetts, 2019) (ver. 3.0, January 2023)*. U.S. Geological Survey Data Release. https://doi.org/10.5066/P915E8JY

Morgan, A. M., & O'Sullivan, A. M. (2022). Cooler, bigger; warmer, smaller: Fine-scale thermal heterogeneity maps age class and species distribution in behaviourally thermoregulating salmonids. *River Research and Applications*, *39*, 163–176. https://doi.org/10.1002/rra.4073

Nichols, W. D. (1994). Groundwater discharge by phreatophyte shrubs in the Great Basin as related to depth to groundwater. *Water Resources Research*, *30*, 3265–3274.

Ocampo, C. J., Oldham, C. E., & Sivapalan, M. (2006). Nitrate attenuation in agricultural catchments: Shifting balances between transport and reaction. *Water Resources Research*, *42*, 1–16. https://doi.org/10.1029/2004WR003773

Olcott, P. G. (1995). Connecticut, Maine, Massachusetts, New Hampshire, New York, Rhode Island, Vermont, HA 730-M. In *Groundwater Atlas of the US*. United States Geological Survey.

Ransom, K. M., Nolan, B. T., Stackelberg, P. E., Belitz, K., & Fram, M. S. (2022). Machine learning predictions of nitrate in groundwater used for drinking supply in the conterminous United States. *Science of the Total Environment*, *807*, 151065. https://doi.org/10.1016/j.scitotenv.2021.151065

Revelli, R., Boano, F., Camporeale, C., & Ridolfi, L. (2008). Intra-meander hyporheic flow in alluvial rivers. *Water Resources Research*, *44*, 1–10. https://doi.org/10.1029/2008WR007081

Rhodes, K. A., Proffitt, T., Rowley, T., Knappett, P. S. K., Montiel, D., Dimova, N., Tebo, D., & Miller, G. R. (2017). The importance of bank storage in supplying baseflow to rivers flowing through compartmentalized, alluvial aquifers. *Water Resources Research*, *53*(12), 10539–10557. https://doi.org/10.1002/2017WR021619

Rice, K. C., & Hornberger, G. M. (1998). Comparison of hydrochemical tracers to estimate source contributions to peak flow in a small, forested, headwater catchment. *Water Resources Research*, *34*, 1755–1766.

Rosenberry, D. O., Briggs, M. A., Voytek, E. B., & Lane, J. W. (2016). Influence of groundwater on distribution of dwarf wedgemussels (*Alasmidonta heterodon*) in the upper reaches of the Delaware River, northeastern USA. *Hydrology and Earth System Sciences*, *20*, 1–17. https://doi.org/10.5194/hess-20-1-2016

Rosenberry, D. O., Sheibley, R. W., Cox, S. E., Simonds, F. W., & Naftz, D. L. (2013). Temporal variability of exchange between groundwater and surface water based on high-frequency direct measurements of seepage at the sediment-water interface. *Water Resources Research*, *49*, 2975–2986. https://doi.org/10.1002/wrcr.20198

Rosenberry, D. O., & Winter, T. C. (1997). Dynamics of water-table fluctuations in an upland between two prairie-pothole wetlands in North Dakota. *Journal of Hydrology*, *191*, 266–289.

Scanlon, B. R., Fakhreddine, S., Rateb, A., de Graaf, I., Famiglietti, J., Gleeson, T., Grafton, R. Q., Jobbagy, E., Kebede, S., Kolusu, S. R., Konikow, L. F., Long, D., Mekonnen, M., Schmied, H. M., Mukherjee, A., MacDonald, A., Reedy, R. C., Shamsudduha, M., Simmons, C. T., … Zheng, C. (2023). Global water resources and the role of groundwater in a resilient water future. *Nature Reviews Earth & Environment*, *1–15*, 2023–2101. https://doi.org/10.1038/s43017-022-00378-6

Schaper, J. L., Zarfl, C., Meinikmann, K., Banks, E. W., Baron, S., Cirpka, O. A., & Lewandowski, J. (2022). Spatial variability of radon production rates in an alluvial aquifer affects travel time estimates of groundwater originating from a losing stream. *Water Resources Research*, *58*(4), 1–22. https://doi.org/10.1029/2021WR030635

Shanafield, M., Cook, P. G., Gutiérrez-Jurado, H. A., Faux, R., Cleverly, J., & Eamus, D. (2015). Field comparison of methods for estimating groundwater discharge by evaporation and evapotranspiration in an arid-zone playa. *Journal of Hydrology*, *527*, 1073–1083. https://doi.org/10.1016/j.jhydrol.2015.06.003

Shapiro, A. M., & Day-Lewis, F. D. (2021). Estimating and forecasting time-varying groundwater recharge in fractured rock: A state-space formulation with preferential and diffuse flow to the water table water resources research. *Water Resources Research*, *57*. https://doi.org/10.1029/2020WR029110

Shapiro, A. M., & Day-Lewis, F. D. (2022). Reframing groundwater hydrology as a data-driven science. *Groundwater*, *60*, 455–456. https://doi.org/10.1111/gwat.13195

Shuai, P., Chen, X., Song, X., Hammond, G. E., Zachara, J., Royer, P., Ren, H., Perkins, W. A., Richmond, M. C., & Huang, M. (2019). Dam operations and subsurface hydrogeology control dynamics of hydrologic exchange flows in a regulated river reach. *Water Resources Research*, *55*, 2593–2612. https://doi.org/10.1029/2018WR024193

Singha, K., & Navarre-Sitchler, A. (2021). The importance of groundwater in critical zone science. *Groundwater*, *60*, 27–34. https://doi.org/10.1111/gwat.13143

Sohn, R. A., & Harris, R. N. (2021). Spectral analysis of vertical temperature profile time-series data in Yellowstone lake sediments. *Water Resources Research*, *57*, 1–25. https://doi.org/10.1029/2020WR028430

Springer, A. E., Boldt, E. M., & Junghans, K. M. (2017). Local vs. regional groundwater flow delineation from stable isotopes at Western North America Springs. *Ground Water*, *55*, 100–109. https://doi.org/10.1111/gwat.12442

Sullivan, C., Vokoun, J., Helton, A., Briggs, M. A., & Kurylyk, B. (2021). An ecohydrological typology for thermal refuges in streams and rivers. *Ecohydrology*, *14*. https://doi.org/10.1002/eco.2295

Sun, L., Seidou, O., Nistor, I., & Liu, K. (2016). Review of the Kalman-type hydrological data assimilation. *Hydrological Sciences Journal*, *61*, 2348–2366. https://doi.org/10.1080/02626667.2015.1127376

U.S. Geological Survey. (2023). *USGS water data for the Nation*. U.S. Geological Survey National Water Information System database. https://doi.org/10.5066/F7P55KJN

White, E. A., Johnson, C. D., Briggs, M. A., Adams, R. F., Stocks, S. J., Minsley, B. J., Kress, W. H., Rigby, J. R., & Lane, J. W. (2020). *Floating and towed transient electromagnetic surveys used to characterize the hydrogeology underlying rivers and estuaries: March–December 2018*. U. S. Geological Survey – Base Data Release. https://doi.org/10.5066/P9E5JBAF

Young, P. C., Taylor, C. J., Tych, W., Pegregal, D. J., & McKenna, P. G. (2010). *The captain toolbox*. Centre for Research on Environmental Systems and Statistics.

Zhi, W., & Li, L. (2020). The shallow and deep hypothesis: Subsurface vertical chemical contrasts shape nitrate export patterns from different land uses. *Environmental Science & Technology*, *54*, 11915–11928. https://doi.org/10.1021/acs.est.0c01340

How to cite this article: Haynes, A. B., Briggs, M. A., Moore, E., Jackson, K., Knighton, J., Rey, D. M., & Helton, A. M. (2023). Shallow and local or deep and regional? Inferring source groundwater characteristics across mainstem riverbank discharge faces. *Hydrological Processes*, *37*(7), e14939. https://doi.org/10.1002/hyp.14939